Journal of Control, Automation and Electrical Systems (2022) 33:1466–1476
https://doi.org/10.1007/s40313-022-00918-x

Euclidean Distance-Based Method for Fault Detection and Classification in Transmission Lines

Guilherme T. Alencar[1] · **Ricardo C. Santos**[1] · **Aline Neves**[1]

Received: 21 February 2021 / Revised: 7 December 2021 / Accepted: 23 February 2022 / Published online: 29 April 2022

Abstract
Overhead transmission lines are the most vulnerable components in electrical power systems. Therefore, to improve the electrical system availability and reliability, fault location should be performed as quickly and accurately as possible. This procedure consists of several steps, including fault detection and classification, which are essential to successfully locate the fault. Due to the importance of these two steps in protection schemes, different approaches have been proposed recently, such as algorithms based on Fourier Transform, Wavelet Transform, Statistical and Artificial Intelligence Techniques. Although they are all promising, they require complex formulations or high computational efforts. This paper proposes a method based on the Euclidean distance measure to perform the fault detection and classification functions, only by using voltage signals from the transmission line ends. The proposed method is simple and robust, not requiring complex formulation or significant computational effort. A large number of tests were performed, considering the power system under different operational conditions and fault characteristics such as fault resistance and fault inception angle, among others. The observed results showed that the proposed method is capable of accurately detecting and classifying faults, regardless of the power system condition or fault characteristic. The comprehensiveness and applicability of the proposed method was confirmed by means of two different transmission lines (line parameters, voltage level, and AC equivalent systems).

Keywords Fault detection · Fault classification · Fault location · Transmission line protection · Euclidean distance · Digital relay

1 Introduction

Accurate performance and high reliability of electric power systems (EPS) are fundamental for the continuity of the electric power supply. However, power interruptions for consumers can occur due to several factors, related to different equipment of the power grid. Due to their extension and exposure, transmission lines (TL) are the most vulnerable components in EPS (Coury et al., 2007).

TL faults can occur for many reasons, for example, weather conditions (rain, snow, wind, etc.), lightning, insulation failures, short circuits caused by birds, trees, among others. In general, the EPS restoration can be accelerated if the fault location is known or estimated with reasonable accuracy. Algorithms for fault location have been developed, thus allowing repairing and restoring the EPS as soon and accurately as possible (Saha et al., 2010). Depending on the used method, the fault locator is composed by different steps. Nonetheless, most of them rely on two essential steps, i.e., fault detection (FD) and fault classification (FC).

Fault detection and classification steps in a TL are of great importance in EPS operation, and they precede the fault location estimation. Different implementation of these steps can be found in practice, most of which are performed in digital relays installed in power substations. Usually, such relays process voltage signals and/or current signals from the TL ends, being able to decide on the TL condition (fault or no-fault) and, in case of fault, discriminate the phases involved. Due to the importance of this topic, over the last years many research groups have been working to improve the fault detection and classification steps. With respect to TL protection, in Saha et al. (2010) and Raza et al. (2020) the authors make a review of the literature, discussing traditional techniques and more complex techniques based on Artificial Intelligence (AI). In order to properly contextual-

✉ Guilherme T. Alencar
alencar.guilherme@ufabc.edu.br

[1] Federal University of ABC, Santo André, Brazil

ize and justify this work, a brief review about fault detection and classification in TL will be presented.

A digital distance relay contains several functions, among them fault detection and classification, which should be simple for a fast and reliable TL protection. According to Coury et al. (2007), fault detection can be done by current sample-by-sample methods, using comparative or estimative algorithms.

Nevertheless, there are more sophisticated methods, based on statistical approaches, for example. In Dubey et al. (2011), authors propose a fault detector based on Independent Component Analysis (ICA) that reduces the computational burden in real-time applications when compared to other methods. In Biswal (2016), the author presents a fault classification algorithm employing an integrated moving sum of current signals. Other methods that employ cumulative sum (Mohanty et al., 2008; Noori et al., 2011) and adaptive cumulative sum (Noori & Shahrtash, 2012, 2013) also take statistical approaches.

In addition to the mentioned works, time–frequency analysis-based methods are also widely used with reasonable accuracy, mainly due to the high sampling rate employed. The wavelet transform (WT) is a widely used tool (Biswas et al., 2018; Costa, 2014; Gautam et al., 2018) due to its ability to work in time–frequency domain. Other methods using S-Transform, that overcomes some disadvantages of the Wavelet Transform, can be found in the literature (Chavez et al., 2021; Mondal et al., 2020).

With the popularization of AI, the amount of works employing this kind of approach in EPS has become greater. Among the various alternatives, it is possible to find works that use Artificial Neural Networks (Abdullah, 2018; Silva et al., 2006; Zhang et al., 2015), Fuzzy Logic (Adhikari et al., 2016; Eboule et al., 2018), Neuro-Fuzzy Systems (Singh et al., 2017; Veerasamy et al., 2018), Support Vector Machine (Jafarian & Sanaye-Pasand, 2013; Johnson & Yadav, 2017) and Baysian Classifier (Jia, 2017; Pérez et al., 2011). The advantages of using these techniques are their ability for pattern recognition and their speed for handling large amounts of data.

In Prasad and Nayak (2019), authors present a method based on the Euclidean Distance between successive current samples for fault detection and classification in TL. According to this reference, current phasors are estimated by using DFT and the decision process is done sample-by-sample. After a large number of tests, the results revealed that the method is reliable and has a low response time. The sampling rate used in this method is 1 kHz.

As discussed above, most proposals use sophisticated algorithms and/or require significant computational effort to perform the fault detection and classification steps. Therefore, the objective of this paper is to present a simple, robust and accurate Euclidean Distance-based method, where only voltage signals and simple operations are used. This means that more sophisticated approaches, involving more computational efforts, can be considered for other steps, for example, the fault location step.

The use of Euclidean distance is not a new issue in classification problems (Hamacher & Nickel, 1998; Kintali et al., 2019; Prasad & Nayak, 2019; Saito & Toriwaki, 1994). However, the use of this concept associated with suitable sampling rates and protection schemes based on voltage traveling waves can bring several advantages, as follows:

- It uses only voltage signal, which is less affected by load and fault conditions. Moreover, the specification of transducers for voltage signals is significantly less critical than for current signals;
- It was tested against fault resistances higher than most of the mentioned references, always presenting an accurate performance;
- It performs fault detection and fault classification demanding a low complexity and computational burden;
- It always responds after half cycle, regardless of the fault condition;
- It works on time domain, not requiring any pre-processing step;
- Communication link is not needed.

This work is organized as follows. In Sect. 2, the main characteristics of the adopted TL are presented, as well as the signals acquisition process. In Sect. 3, the proposed scheme, based on Euclidean Distances, for fault detection and classification is discussed. In Sect. 4, the proposed scheme is evaluated and validated. Finally, the conclusions are drawn in Sect. 5.

2 Adopted TL and Data Acquisition Process

To implement a reliable fault location algorithm, it is important to firstly consider an accurate fault detection and classification scheme. For developing and testing the proposed scheme for fault detection and classification, a TL must be carefully chosen and modeled, allowing the generation of voltage signals representing fault conditions and normal operation.

2.1 Adopted Transmission Line

To develop and evaluate the proposed scheme, a TL of 500 kV (at 60 Hz) and 200 km length was used. The adopted TL and its main parameters are shown in Fig. 1, where V_1, Z_1 V_2 and Z_2 represent the AC equivalent systems connected to the TL ends. After implementing this TL in PSCAD, a large number of simulations were performed considering fault and no-fault cases, thus allowing generating and saving the volt-

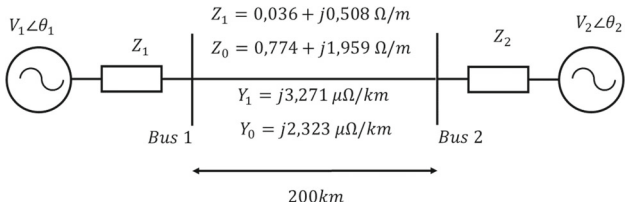

Fig. 1 Adopted TL of 500 kV

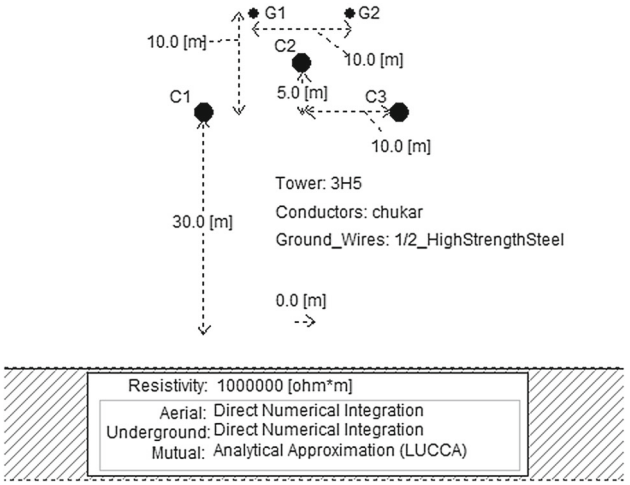

Fig. 2 Tower geometry and conductors characteristics

age signals of interest for this study. It is important to mention that the TL was modeled by using the frequency dependent model, which incorporates the frequency dependence of all parameters, considering the tower geometry and conductors characteristics shown in Fig. 2.

2.2 Data Acquisition Process

Several fault conditions were simulated in the adopted TL, in order to develop and evaluate the proposed method. For each simulated fault condition, the voltage signals were sampled at 100 kHz and the measurements were taken at the bus 1. Nowadays, this sampling frequency is reasonable and significantly lower than many schemes designed for the same purpose. In fact, according to Marx et al. (2013) many schemes use sampling frequencies between 0.5 and 5 MHz.

The sliding data window used by the proposed algorithm has one cycle length and it is updated each half cycle, as shown in Fig. 3. Thus, any disturbance in the TL always will be detected within a half cycle. In this way, the proposed scheme for fault detection continuously monitors the local voltage signals and, in case of fault, the one cycle window containing the fault event is collected to proceed with the fault classification step.

Voltage waveform was chosen as input signal for the proposed scheme, since it has less variation during fault events.

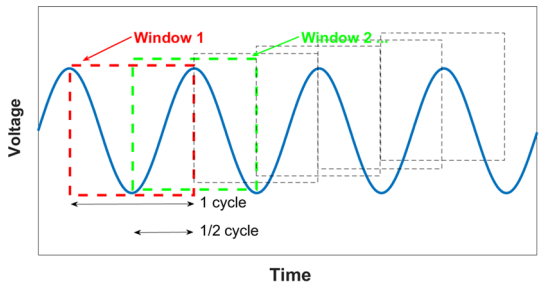

Fig. 3 Sliding data window and its updating process

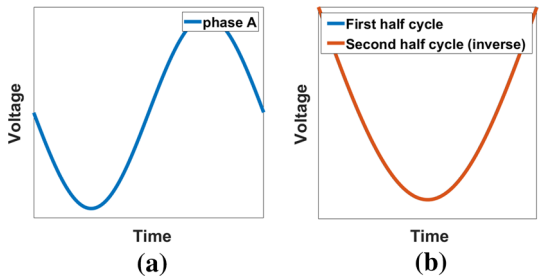

Fig. 4 Voltage signal—EPS under normal condition (no fault). **a** One cycle signal—EPS under normal condition (no fault). **b** Comparison between the first half cycle and the inverted second half cycle

Also, it is less affected by load conditions, differently from the current signal that is strongly affected by load conditions or fault characteristics. In addition, by adopting voltage as input signal, there is no concern about current transformer (CT) saturation, which could lead to misoperation due to distortion on the input signal.

3 Proposed Scheme for Fault Detection and Classification

This section discusses the proposed scheme for fault detection and classification, presenting details about the preprocessing step and the designed protection logic.

3.1 Euclidean Distance in Fault Detection and Classification

As an example, Fig. 4a shows the voltage waveform (Phase A and bus 1) measured at the local end of the TL shown in Fig. 1, which represents one cycle at 60 Hz. Since it is a periodic signal, the comparison between the first half cycle and the second inverted half cycle is ideally null, as shown in Fig. 4b. On the other hand, Fig. 5a shows the voltage waveform (Phase A and bus 1) when a fault occurs at some point on the second half cycle. Unlike the previous case (Fig. 4), the difference between the first half cycle and the inverted second half cycle is not null (Fig. 5b), clearly indicating a disturbance in the EPS.

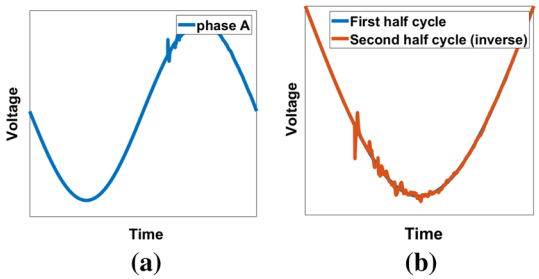

Fig. 5 Voltage signal—EPS under fault. **a** One cycle after a fault. **b** Comparison between the first half cycle and the second half cycle of a fault phase

The lack of similarity between both curves presented in Fig. 5 can be estimated by using Euclidean distance, thus acting as a parameter for detecting TL disturbances. In this sense, consider a voltage signal represented by the vector $V_1 = \left[\, v[1] \cdots v[N] \,\right]$, where $v[n]$ represents the nth sample of the voltage signal and N corresponds to total number of samples, i.e., a full cycle of voltage. The vector V is divided into two semi-cycles with the same time interval, according to Eqs. (1) and (2).

$$V_1 = \left[\, v[1] \cdots v\left[\tfrac{N}{2}\right] \right] = \left[\, v_1[1] \cdots v_1\left[\tfrac{N}{2}\right] \right] \tag{1}$$

$$V_2 = \left[\, v\left[\tfrac{N}{2}+1\right] \cdots v[N] \right] = \left[\, v_2[1] \cdots v_2\left[\tfrac{N}{2}\right] \right] \tag{2}$$

The Euclidean distance between the first half cycle and the inverted second half cycle can be calculated according to (3).

$$dist = \|V_1 + V_2\| = \sqrt{\sum_{k=1}^{N/2} (v_1[k] + v_2[k])^2} \tag{3}$$

where $\|\cdot\|$ corresponds to the Euclidean norm.

Assuming that this proposal uses three-phase voltage signals, Eq. (3) can be rewritten per phase, according to Eq. (4), where ph can be replaced by phases a, b and c.

$$dist_{ph} = \left\| V_{ph1} + V_{ph2} \right\| \tag{4}$$

3.2 Fault Detection

The objective in defining the Euclidean distance given by Eq. (4) is to measure the level of disturbance of each phase. When there is no disturbance or when the disturbance is not significant, $dist_{det}$ will be lower than a threshold value and so a fault condition is not recognized. However, for more significant disturbances, the Euclidean distance will be higher than a threshold value and so a fault condition is detected. In an EPS operating with three-phase voltages, Eq. (5) can be used as a reference for disturbances detection.

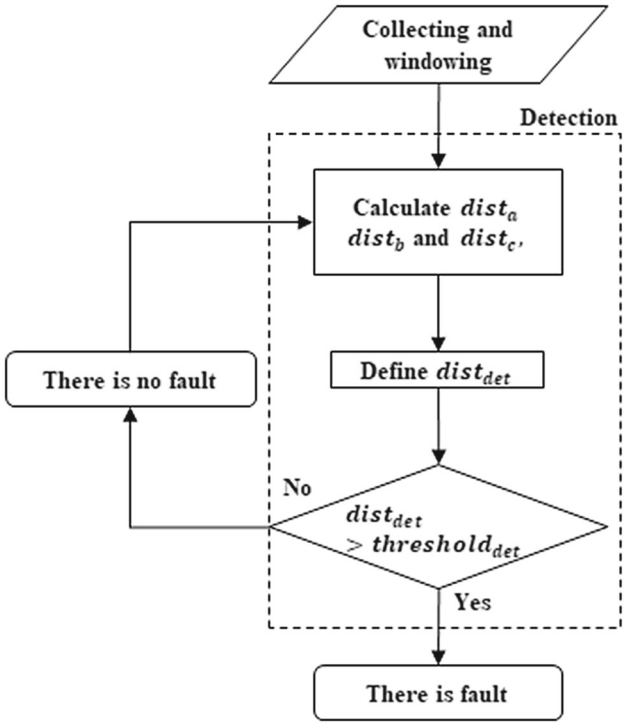

Fig. 6 Flowchart for fault detection

$$dist_{det} = maximum(dist_a, dist_b, dist_c) \tag{5}$$

where $dist_a$, $dist_b$ and $dist_c$ correspond to the value of $dist_{ph}$ for phases a, b and c, respectively, according to Eq. (4).

The proposed fault detection scheme calculates $dist_{det}$ after each new updating, i.e., each half cycle of voltage signal. In order to declare the existence of a fault, a detection threshold $threshold_{det}$ is defined to differentiate between normal and fault conditions. Thus, if $dist_{det} > threshold_{det}$, there is a fault in the analyzed data window; otherwise, it does not exist. The flowchart in Fig. 6 shows the fault detection step.

To precisely declare a fault condition, it is necessary to define the value of $dist_{det}$ (5), which allows the differentiation between a fault condition and a normal operational condition. In order to exemplify the operation of the fault detection scheme, Fig. 7 shows the voltage signal for a fault condition close to the middle of the data window. At the end of each half cycle, values of $dist_{det}$ are calculated and a decision is made by the proposed scheme, as can be seen by the blue bars. This procedure is in accordance to the explanation given when discussing Fig. 3. Note that pre-fault $dist_{det}$ values are compared to post-fault values. When post-fault values exceed a pre-defined threshold, the fault is detected inside this data window, and the signals are collected for the following steps. After several simulations, with various

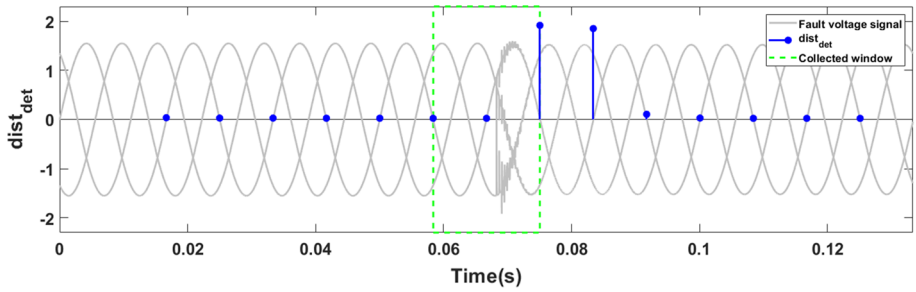

Fig. 7 Fault detection response and windowing process

fault and normal conditions, the value of 0.1 was defined as a threshold for fault detection.

It is important to mention that to distinguish lightning and switching occurrences from fault events an additional protection logic could be implemented so that a possible misoperation of the protection scheme can be avoided.

3.3 Fault Classification

The Euclidean distance $dist_{ph}$ can also be used to indicate in which phases the fault occurred and, consequently, to classify the faults in the TL. To build an accurate fault classifier, the threshold values $dist_{ph}$ are not enough, since faults in one phase can influence the other phases. In addition, since TL faults can involve ground, Eq. (6) is used to signalize this involvement, comparing $dist_g$ value with a threshold value, defined as $threshold_g$ (ground threshold). If ground is involved, the fault may be line-ground (L-G) or line-line-ground (L-L-G). Otherwise, the fault can be line-line (L-L) or line-line-line (L-L-L).

$$dist_g = \|(V_{a1} + V_{b1} + V_{c1}) + (V_{a2} + V_{b2} + V_{c2})\| \tag{6}$$

After verifying the ground involvement, it is defined which phases have the highest value, lowest value and median value of Euclidean distance, according to Eqs. (7)–(9), which will be used to define the faulty phases.

$$dist_{ph}^{max} = maximum(dist_a, dist_b, dist_c) \tag{7}$$

$$dist_{ph}^{min} = minimum(dist_a, dist_b, dist_c) \tag{8}$$

$$dist_{ph}^{med} = median(dist_a, dist_b, dist_c) \tag{9}$$

Discarding the ground involvement and since at least two phases are involved (because they can only be L-L or L-L-L), the classification of these two types of fault consists of determining whether the phase with the shortest Euclidean distance participates in the fault. In other words, the phase of Eq. (8) is calculated and so this value is compared with a threshold value, defined as $threshold_{(LL/LLL)}$. This threshold can be determined according to Eq. (10), as a function of the detection threshold.

$$threshold_{(LL/LLL)} = k \cdot threshold_{det} \tag{10}$$

where k is a constant.

If $dist_{ph}^{min} > threshold_{(LL/LLL)}$, then the phase with the shortest Euclidean distance participates in the fault, otherwise not. Simulations in this work were run for two TL models (500 kV and 440 kV), as will be shown later. After 78 fault cases for each TL the value of $k = 1$ proved to be quite opportune.

For faults involving ground (L-G and L-L-G), a more refined method is necessary, as the healthy phases are also significantly affected. First, the classification distances must be normalized, by calculating the phases with the shortest and longest Euclidean distance, according to (11) and (12), respectively, emphasizing that the ground component should be considered. The distance of the *ph-th* normalized phase is determined according to Eq. (13).

$$dist^{min} = minimum\big(dist_a, dist_b, dist_c, dist_g\big) \tag{11}$$

$$dist^{max} = maximum\big(dist_a, dist_b, dist_c, dist_g\big) \tag{12}$$

$$dist_{ph(norm)} = \frac{dist_{ph} - dist^{min}}{dist^{max} - dist^{min}} \tag{13}$$

As it is a single-phase or double-phase fault, one of the phases is involved and the other is not, remaining to determine whether the phase with a median distance, called $dist_{ph(norm)}^{med}$ (Eq. (14)) is under fault condition or not. In L-G faults, median distance tends to be close to zero, while in L-L-G faults it tends to be close to one. Therefore, it is possible to assign the condition of $dist_{ph(norm)}^{med} > 50\%$ for double-phase faults and $dist_{ph(norm)}^{med} < 50\%$ for single-phase faults.

$$dist_{ph(norm)}^{med} = median\big(dist_{a(norm)}, dist_{b(norm)}, dist_{b(norm)}\big) \tag{14}$$

The flowchart in Fig. 8 summarizes the fault classification step.

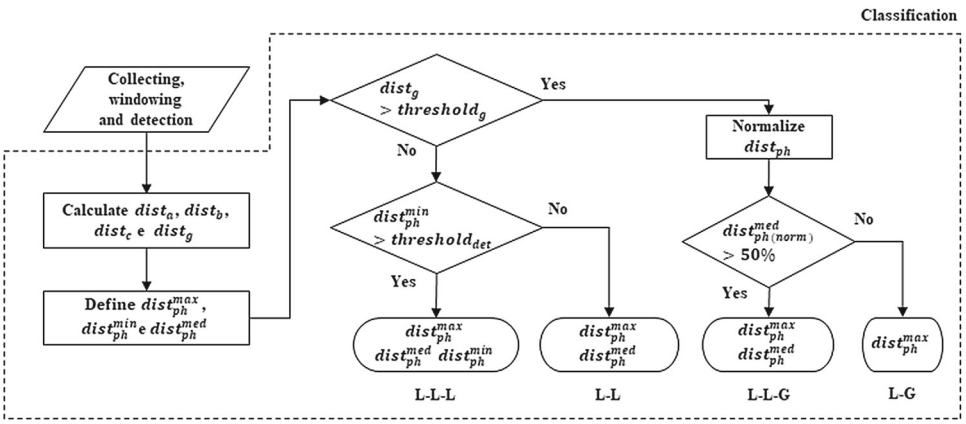

Fig. 8 Flowchart for fault classification

4 Proposed Method Evaluation

The results obtained with the proposed scheme for fault detection and classification are analyzed and discussed in this section. In addition to the TL shown in Fig. 1 (500 kV and 200 km LT), a second TL was also modeled and simulated. This second one has voltage level of 440 kV and 330 km length, which represents a significant difference when compared to the first one. In this way, it will be possible to evaluate the proposed scheme under many operational conditions and considering two different TL, giving the results greater credibility.

4.1 Cases considering the TL of 500 kV

The TL adopted for this evaluation was modeled in PSCAD, where several fault cases were simulated and analyzed. To evaluate the proposed scheme, many fault conditions were generated by changing the following parameters: fault location, fault type, fault resistance, fault inception angle, and bus voltage. As depicted in Table 1, 78 fault cases were simulated and the voltage waveforms at the bus 1 were stored, thus allowing a later implementation of the fault detection and classification steps in MATLAB. The fault cases were simulated assuming solid and non-solid faults, as shown in Table 1.

4.2 Results for fault detection—TL of 500 kV

The procedure described in the flowchart presented in Fig. 6 was applied in all 78 fault cases, and their correspondents $dist_{det}$ values are shown in Fig. 9. As can be seen, for all considered fault cases the Euclidean distances are higher than the chosen threshold, accurately indicating the fault.

Table 2 shows the average value of $dist_{det}$ with respect to Fig. 9. As can be seen, the selected threshold was always able to detect faults, even against high values of fault resistance.

Table 1 Adopted power system and faults characteristics

Feature	Considered values
Fault location (distance from bus 1 in km)	from 5 to 195 (steps = 5 km)
Fault type	A; B; C; AB; AC; BC; ABT; ACT; BCT; ABC
Fault resistence (Ω)	0; 50 and 100
Fault incidence angle (°)	− 90; − 60; − 30; 0; 30; 60; 90
Voltage at bus 1 (pu)	1; 1.05
Voltage at bus 2 (pu)	1
Angle at bus 2 (°)	− 5; − 10
Inductance at bus 1 and bus 2 (mH)	5

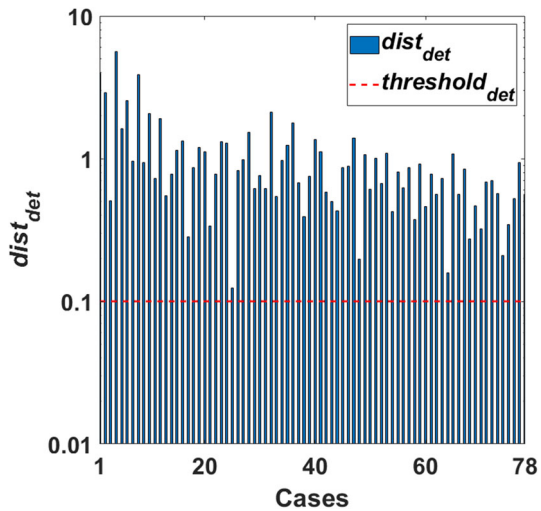

Fig. 9 $dist_{det}$ values for fault detection—TL of 500 kV

4.3 Results for fault classification—TL of 500 kV

To perform the fault classification step, the procedure showed in Fig. 8 was applied. After calculating the Euclidean distances for each phase, the Euclidean distance for ground

Table 2 Average value of $dist_{det}$—TL of 500 kV

Cases	Average $dist_{det}$
Solid faults R	1.35
Non-solid faults R	0.68
All faults	1.01

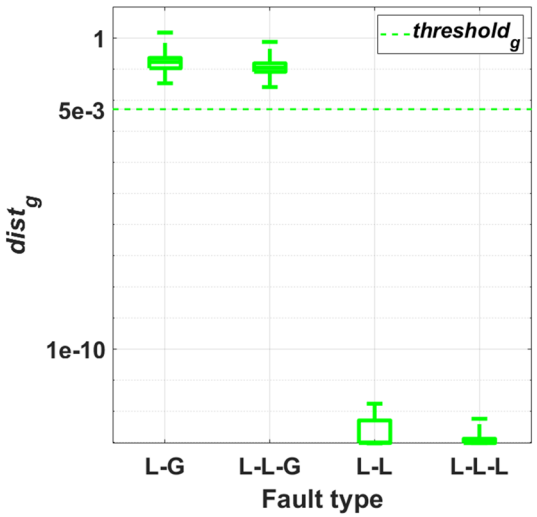

Fig. 10 $dist_g$ values for fault classification—TL of 500 kV

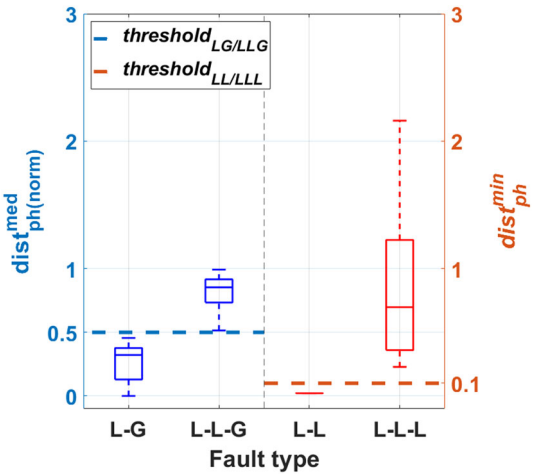

Fig. 11 Distance values for fault classification—TL of 500 kV

Table 3 Observed values for $dist^{med}_{ph(norm)}$ and $dist^{min}$—TL of 500 kV

Cases	Average	Minimum	Maximum
L-G	0.26	0.00	0.45
L-L-G	0.82	0.51	0.99
L-L	0.02	0.02	0.02
L-L-L	0.93	0.7	2.07

involvement was also calculated to determine the type of fault (6)–(9). All fault cases were grouped according to the fault type by using boxplot, as shown in Fig. 10.

By defining a ground threshold of 0.005, it is possible to observe that the first two groups of faults have a ground Euclidean distance above the threshold, while the last two ones have values below that threshold. Therefore, results show that ground Euclidean distance value is able to discriminate between faults involving ground and not involving ground. In this way, it is possible to proceed with the next step of fault classification, determining which Euclidean distance will be calculated for fault classification: $dist^{min}_{ph}$ or $dist^{med}_{ph(norm)}$, defined in Eqs. (8) and (14), respectively.

Figure 11 shows the results for fault classification, where the cases are grouped by using bloxplot graph. The left vertical axis shows the calculated values of $dist^{med}_{ph(norm)}$ (in blue) according to Eq. (14) that evaluates whether the faults are L-G or L-L-G. The right vertical axis (in red) shows the values of $dist^{min}_{ph}$ as defined in Eq. (14), which assesses whether the faults are L-L or L-L-L. Table 3 shows the average, minimum and maximum values of each boxplot in Fig. 11.

It is clearly noted that all fault cases were correctly classified according to the missing phase, since the thresholds defined in Sect. 3.3 correctly classified the fault types. For the left fault group (in blue), the calculated median distances below the threshold indicate that there is only one phase involved, while distances that present values above the threshold indicate two phases involved. Considering the group of faults on the right (in red), cases that present classification distance values below the threshold indicate that the cases involve two phases and cases that present distances above the threshold indicate that all the three phases are involved.

As can be seen in Fig. 11 and Table 3, some few cases are close to the threshold values. However, it is worth mentioning that the proposed method was always able to correctly classify the fault, considering the ranges defined in Table 1 and 78 fault cases simulated.

4.4 Cases considering the TL of 440 kV

To validate and give more credibility to results and analyzes obtained in the previous sections, a second TL was modeled and simulated considering several faults conditions. This second TL (Figs. 12, 13) differs from the previous one with respect to the tower geometry, voltage level (440 kV) and line length (330 km). Also, by means of this procedure, it will be possible to reevaluate the threshold values previously defined.

Once again, 78 fault cases were generated by changing the parameters depicted in Table 1. It is important to mention that the only difference, when compared to the first TL, is the fault location, which now varies from 10 to 320 km away from bus 1. This measure aims to provide a greater variety of fault

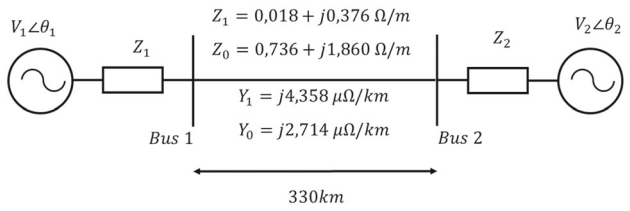

Fig. 12 Adopted TL of 440 kV

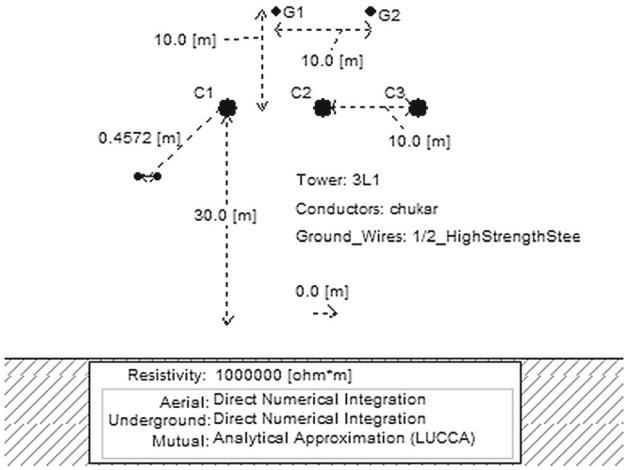

Fig. 13 Tower geometry and conductors characteristics

Table 4 Average value of $dist_{det}$—TL of 440 kV

Cases	Average $dist_{det}$
Solid faults *R*	1.50
Non-solid faults *R*	0.60
All faults	1.05

cases to perform this study, showing the comprehensiveness of the proposed solution.

4.5 Results for fault detection—TL of 440 kV

To evaluate the fault detection step, the same procedure described in the flowchart shown in Sect. 3.2 was performed. The detection distance values for all simulated fault cases are shown in Fig. 14, recalling that the same threshold previously defined was used. As can be seen, for all simulated fault cases the calculated distance values are above the defined threshold, indicating that the detection algorithm is effective for several TL models. Similarly to Table 2, the average values of $dist_{det}$ are presented in Table 4, confirming the threshold value previously defined for fault detection.

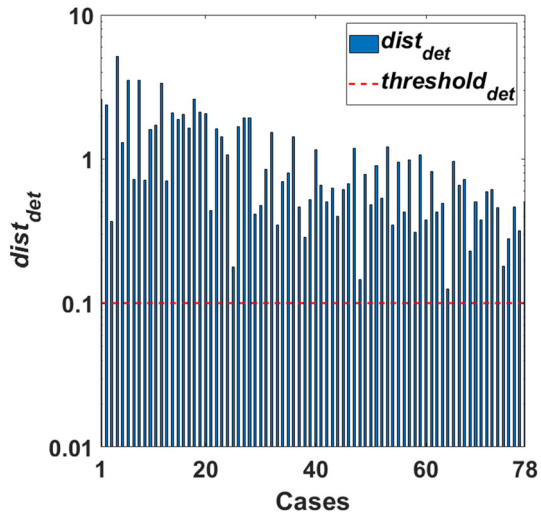

Fig. 14 $dist_{det}$ for fault detection—TL of 440 kV

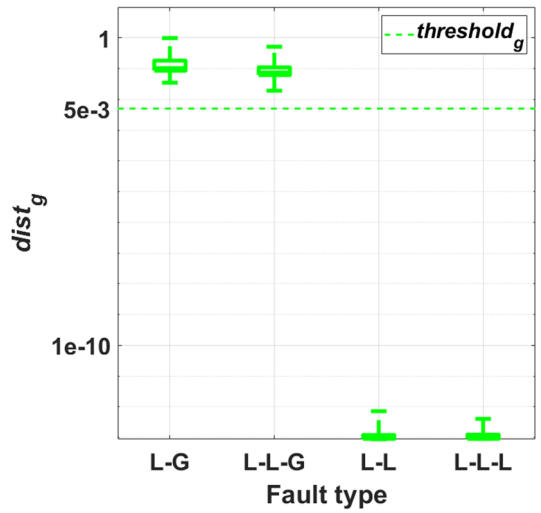

Fig. 15 $dist_g$ values for fault classification—TL of 440 kV

4.6 Results for fault classification—TL of 440 kV

The proposed classification scheme was also evaluated against the TL of 440 kV. Initially, the step that defines ground involvement was applied to group the faults cases in L-G/L-L-G or L-L/L-L-L. Similar to Fig. 10, this step results are shown in Fig. 15, where it is observed that the same threshold used in the previous TL was able to indicate faults with ground involvement.

The step for distances calculation, defined in Eqs. (8) and (14), was applied to classify faults considering faults with and without ground involvement. The results are shown in Fig. 16 by means of a boxplot, similar to the procedure adopted for Fig. 11. The same thresholds previously defined (TL of 500 kV) were used. The results showed that the proposed scheme correctly responds regardless the adopted TL,

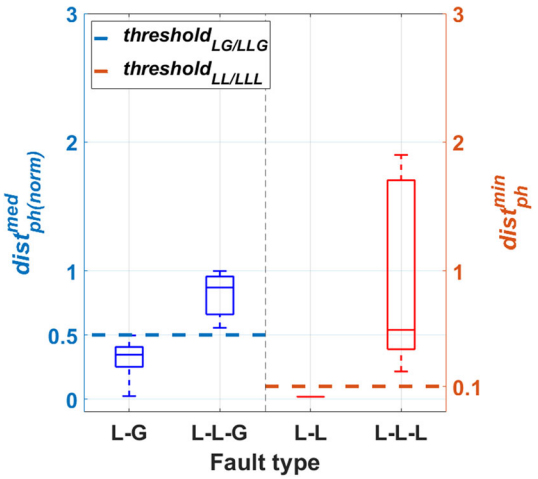

Fig. 16 Distance values for fault classification—TL of 440 kV

Table 5 Observed values for $dist^{med}_{ph(norm)}$ and $dist^{min}$—TL of 440 kV

Cases	Average	Minimum	Maximum
L-G	0.30	0.00	0.49
L-L-G	0.82	0.56	0.98
L-L	0.02	0.02	0.02
L-L-L	0.91	0.22	1.83

operating conditions, fault locations, type of fault and fault resistance. Once again, as can be seen in Fig. 16 and Table 5, some few fault cases are close to the defined thresholds. Nevertheless, for all 78 simulated fault cases, considering the ranges shown in Table 1, the proposed method performed as expected, properly classifying the fault.

4.7 Performance comparison

To compare the proposed Euclidean distance-based method with other methods found in the literature, Table 6 is presented. As can be seen, this table allows comparisons regarding factors as input signals, used algorithm, test systems, sampling frequency, response time, and complexity.

By analyzing Table 6, it can be seen that the main advantages of the proposed method are as follows: (a) it uses only voltage signals, which are less affected by load and fault conditions. Moreover, the specification of transducers for voltage signals (PT) is less critical than for current signals (CT), as voltage works in a narrower operating range; (b) communication link is not needed; (c) two different transmission lines were used during its evaluation step; (d) it is able to perform FD and FC requiring low computational burden; (e) it works on time domain, not requiring any pre-processing step. Even though the sampling rate of the proposed method is higher than the ones used by most of the other methods, it is still reasonable.

In terms of response time, Prasad and Nayak (2019) and Pérez et al. (2011) are faster than the proposed method, but their accuracies are guaranteed for fault resistances up to 50 Ω and 40 Ω, respectively, while the proposed method is accurate up to 100 Ω. On the other hand, the method developed by Gupta and Tripathy (2015) presents a good performance up to 500 Ω, with a reasonable response time. Nevertheless, this method uses two variables (V and I) and needs a communication link, making the protection design more complex and expensive.

It is important to highlight that differently from the other methods, the proposed one was tested against two different transmission lines, considering a large number of fault cases and operating conditions. By means of hundreds of simulations the proposed method proved to be a feasible and reliable option for fault detection and classification in transmission lines.

5 Conclusions

In this paper, a Euclidean distance-based method was proposed for fault detection and classification in TL. Several fault cases were simulated to evaluate the proposed method against two different TL and fault characteristics. The observed results showed that for all considered fault cases (78 for each TL), the proposed method was able to correctly detect and classify the fault, regardless the operational condition or fault characteristics (fault location, fault resistance and fault inception angle).

For detection and classification purposes, the method is based on the similarity level between two consecutives half cycles, estimated by using Euclidean distance. This feature makes the proposed method easy to implement for practical applications, as the required computational effort is very low when comparing with most of the other methods. Moreover, the solution presented here does not need communication link or any pre-processing step, correctly responding for fault resistances up to 100 Ω.

The comprehensiveness and robustness of the proposed method was proved by means of two different TL. It is worth noting that even keeping the same threshold values, the expected performance was observed in both situations.

Table 6 Comparison between different methods for fault detection and classification

References	Algorithm	Input signal	Test system	Fault resistance (Ω)	Complexity	Sampling frequency (kHz)	Performed function	Response time
Proposed method	Euclidean distance (time domain)	V	500 kV, 200 km, and 440 kV, 330 km	100	Low	100	FD and FC	HC
Prasad and Nayak (2019)	Euclidean Distance (Frequency domain)	I	230 kV, 300 km	50	Low	1	FD and FC	<HC
Kintali et al. (2019)	Euclidean distance (time domain)	I	400 kV, 300 km	50	Low	1	FD and FC	HC
Yadav and Sweta-padma (2015)	Linear Discriminant Analysis and Wavelet Transform	I	400 kV, 100 km	100	Moderate	1	FD and FC	OC
Gupta and Tripathy (2015)	Superimposed Sequence Components based integrated impedance	V and I from both terminals	400 kV, 300 km	500	High	1	FD	<OC
Pérez et al. (2011)	Bayesian classifier and adaptive wavelet	I	500 kV, 864 km	40	High	500	FD and FC	<HC

HC half cycle, *OC* one cycle, *V* voltage, *I* current

References

Abdullah, A. (2018). Ultrafast transmission line fault detection using a DWT-based ANN. *IEEE Transactions on Industry Applications, 54*, 1182–1193. https://doi.org/10.1109/TIA.2017.2774202

Adhikari, S., Sinha, N., & Dorendrajit, T. (2016). Fuzzy logic based on-line fault detection and classification in transmission line. *Springerplus, 5*, 1002. https://doi.org/10.1186/s40064-016-2669-4

Biswal, M. (2016). Faulty phase selection for transmission line using integrated moving sum approach. *IET Science, Measurement and Technology, 10*, 761–767. https://doi.org/10.1049/iet-smt.2016.0081

Biswas, S., Kumar, K., Ghosal, A., & Nayak, P. K. (2018). Fault detection and classification for TCSC compensated transmission lines using wavelet energy. In *2018 4th International Conference on Recent Advances in Information Technology (RAIT)* (pp. 1–5). IEEE.

Chavez, J. J., Popov, M., López, D., et al. (2021). S-Transform based fault detection algorithm for enhancing distance protection performance. *International Journal of Electrical Power & Energy Systems, 130*, 106966. https://doi.org/10.1016/j.ijepes.2021.106966

Costa, F. B. (2014). Fault-induced transient detection based on real-time analysis of the wavelet coefficient energy. *IEEE Transactions on Power Delivery, 29*, 140–153. https://doi.org/10.1109/TPWRD.2013.2278272

Coury, D. V., Oleskovicz, M., & Giovanini, R. (2007). Digital protection of electric power systems: From the electromechanical relays to intelligent microprocessors.

Dubey, H. C., Mohanty, S. R., & Kishore, N. (2011). Abrupt change detection of fault in power system using independent component analysis. In *2011 International conference on signal processing, communication, computing and networking technologies* (pp 659–664). IEEE.

Eboule, P. P., Pretorius, J. H. C., Mbuli, N., & Leke, C. (2018). Fault detection and location in power transmission line using concurrent neuro fuzzy technique. In *2018 IEEE Electrical Power and Energy Conference (EPEC)* (pp. 1–6). IEEE.

Gautam, N., Ali, S., & Kapoor, G. (2018). Detection of fault in series capacitor compensated double circuit transmission line using wavelet transform. In *2018 International conference on computing, power and communication technologies (GUCON)* (pp. 760–764). IEEE.

Gupta, O. H., & Tripathy, M. (2015). An innovative pilot relaying scheme for shunt-compensated line. *IEEE Transactions on Power Delivery, 30*, 1439–1448. https://doi.org/10.1109/TPWRD.2015.2394353

Hamacher, H. W., & Nickel, S. (1998). Classification of location models. *Location Science, 6*, 229–242. https://doi.org/10.1016/S0966-8349(98)00053-9

Jafarian, P., & Sanaye-Pasand, M. (2013). High-frequency transients-based protection of multiterminal transmission lines using the SVM technique. *IEEE Transactions on Power Delivery, 28*, 188–196. https://doi.org/10.1109/TPWRD.2012.2215925

Jia, H. (2017). An improved traveling-wave-based fault location method with compensating the dispersion effect of traveling wave in wavelet domain. *Mathematical Problems in Engineering, 2017*, 1–11. https://doi.org/10.1155/2017/1019591

Johnson, J. M., & Yadav, A. (2017). Complete protection scheme for fault detection, classification and location estimation in HVDC transmission lines using support vector machines. *IET Science, Measurement and Technology, 11*, 279–287. https://doi.org/10.1049/iet-smt.2016.0244

Kintali, M., Sura, S. R., Pulivarthi, N. R., & Kondaji, A. K. (2019). Euclidean metric based fault diagnosis in power transmission line. *International Journal of Innovative Technology and Exploring Engineering, 9*, 226–231. https://doi.org/10.35940/ijitee.B1057.1292S319

Marx, S., Johnson, B., & Guzmán A. (2013). Traveling wave fault location in protective relays: Design, testing, and results. In *16th Annu Georg Tech Fault Disturb Anal Conf Atlanta*, Georg, pp. 1–14.

Mohanty, S. R., Pradhan, A. K., & Routray, A. (2008). A cumulative sum-based fault detector for power system relaying application. *IEEE Transactions on Power Delivery, 23*, 79–86. https://doi.org/10.1109/TPWRD.2007.911160

Mondal, A., Das, S., & Patel, B. (2020). Fault detection during power swing using fast discrete S-transform, pp. 73–79. https://doi.org/10.1007/978-981-13-8687-9_7

Noori, M. R., Jamali, S., & Shahrtash, S. M. (2011). Security assessment for a cumulative sum-based fault detector in transmission lines. In *2011 10th international conference on environment and electrical engineering* (pp. 1–5). IEEE.

Noori MR, Shahrtash SM (2012) A novel faulted phase selector for double circuit transmission lines by employing adaptive cumulative sum-based method. In: 2012 11th International Conference on Environment and Electrical Engineering. IEEE, pp 365–370

Noori, M. R., & Shahrtash, S. M. (2013). Combined fault detector and faulted phase selector for transmission lines based on adaptive cumulative sum method. *IEEE Transactions on Power Delivery, 28*, 1779–1787. https://doi.org/10.1109/TPWRD.2013.2261563

Pérez, F. E., Orduña, E., & Guidi, G. (2011). Adaptive wavelets applied to fault classification on transmission lines. *IET Generation, Transmission and Distribution, 5*, 694. https://doi.org/10.1049/iet-gtd.2010.0615

Prasad, C. D., & Nayak, P. K. (2019). A DFT-ED based approach for detection and classification of faults in electric power transmission networks. *Ain Shams Engineering Journal, 10*, 171–178. https://doi.org/10.1016/j.asej.2018.02.004

Raza, A., Benrabah, A., Alquthami, T., & Akmal, M. (2020). A review of fault diagnosing methods in power transmission systems. *Applied Sciences*. https://doi.org/10.3390/app10041312

Saha, M. M., Izykowski, J., & Rosolowski, E. (2010). *Fault location on power networks*. Springer.

Saito, T., & Toriwaki, J.-I. (1994). New algorithms for euclidean distance transformation of an n-dimensional digitized picture with applications. *Pattern Recognition, 27*, 1551–1565. https://doi.org/10.1016/0031-3203(94)90133-3

Silva, K. M., Souza, B. A., & Brito, N. S. D. (2006). Fault detection and classification in transmission lines based on wavelet transform and ANN. *IEEE Transactions on Power Delivery, 21*, 2058–2063. https://doi.org/10.1109/TPWRD.2006.876659

Singh, S., Vishwakarma, D. N., Kumar, A., & Shashank. (2017). A novel methodology for fault detection, classification and location in transmission system based on DWT & ANFIS. *Journal of Information and Optimization Sciences, 38*, 791–801. https://doi.org/10.1080/02522667.2017.1372129

Veerasamy, V., Abdul Wahab, N., Ramachandran, R., et al. (2018). High impedance fault detection in medium voltage distribution network using discrete wavelet transform and adaptive neuro-fuzzy inference system. *Energies, 11*, 3330. https://doi.org/10.3390/en11123330

Yadav, A., & Swetapadma, A. (2015). A novel transmission line relaying scheme for fault detection and classification using wavelet transform and linear discriminant analysis. *Ain Shams Engineering Journal, 6*, 199–209. https://doi.org/10.1016/j.asej.2014.10.005

Zhang, R., Li, C., & Jia, D. (2015). A new multi-channels sequence recognition framework using deep convolutional neural network. *Procedia Compute Science, 53*, 383–390. https://doi.org/10.1016/j.procs.2015.07.315